Biophysical characterization of SipA, an actin-binding protein from *Salmonella enterica*

Kakoli Mitra[a,1], Daoguo Zhou[b], Jorge E. Galán[b,*]

[a] *Department of Cell Biology, Yale University, New Haven, CT 06510, USA*
[b] *Section of Microbial Pathogenesis, Boyer Center for Molecular Medicine, Yale University School of Medicine, New Haven, CT 06536, USA*

Received 17 August 2000; revised 31 August 2000; accepted 31 August 2000

Edited by Hans Eklund

Abstract An essential step in the pathogenesis of *Salmonella enterica* infections is bacterial entry into non-phagocytic cells of the intestinal epithelium. Proteins injected by *Salmonella* into host cells stimulate cellular responses that lead to extensive actin cytoskeleton reorganization and subsequent bacterial uptake. One of these proteins, SipA, modulates actin dynamics by directly binding to F-actin. We have biophysically characterized a C-terminal fragment, SipA$^{446-684}$, which has previously been shown to retain activity. Our results show that SipA$^{446-684}$ exhibits an elongated shape with a predominantly helical conformation and predict the existence of a coiled-coil domain. We suggest that the protein is able to span two adjacent actin monomers in a filament and propose a model that is consistent with the observed effects of SipA$^{446-684}$ on actin dynamics and F-actin stability and morphology.

Key words: Actin-binding protein; Cytoskeleton; Actin dynamics; *Salmonella enterica*

1. Introduction

Salmonella enterica, the causative agent of a variety of diseases such as typhoid fever or food poisoning, has evolved sophisticated strategies to modulate host cellular functions [1]. One of these strategies allows these bacteria to manipulate the actin cytoskeleton to enter into non-phagocytic cells such as those of the intestinal epithelium [2]. Bacterial internalization is the consequence of the sequential activity of a number of bacterial proteins that are delivered into the host cell by a specialized bacterial organelle termed the type III secretion system [3]. These bacterial proteins include an exchange factor (SopE) [4], a GTPase-activating protein (SptP) [5] for Cdc42 and Rac, an inositol phosphate polyphosphatase (SopB) [6] and an actin-binding protein (SipA) [7]. The combined activity of these bacterial effectors results in the activation of the small molecular weight GTP-binding proteins Cdc42 and Rac and the stimulation of actin cytoskeleton rearrangements that lead to bacterial uptake [2,8–10].

Previous studies have shown that the *Salmonella* SipA protein binds to actin during bacterial infection [7]. In vitro studies have demonstrated that the binding of SipA to F-actin (1:1 molar ratio) has marked effects on actin dynamics, i.e. the concentration of G-actin required for polymerization (critical concentration) is reduced 10-fold (from 0.25 μM to 0.02 μM), and also on F-actin stabilization, i.e. depolymerization of F-actin induced by low ionic strength is inhibited. Furthermore, SipA-binding to actin results in a marked increase in the actin-bundling activity of other actin-binding proteins such as fimbrin [11]. It has been hypothesized that such modulation of the activity of other actin-binding proteins may be the result of the effect of SipA on the structure of the F-actin filament itself [11]. Indeed, electron microscopic studies have shown that the binding of SipA to F-actin leads to a significant straightening of actin filaments, which presumably facilitates the function of actin cross-linking proteins such as fimbrin [11]. Deletion analysis has established that the actin-modulating activity of SipA is contained within the last 238 amino acids (SipA$^{446-684}$), suggesting that the amino-terminal half of this protein may be involved in other biological activities or in the regulation of SipA function in vivo [7]. The biological consequence of SipA activity is a marked increase in the efficiency of bacterial internalization by non-phagocytic cells, since *Salmonella* strains carrying a loss-of-function mutation in *sipA* are significantly reduced in their ability to gain access into host cells [7].

Understanding the precise mechanism of action of SipA is of great interest since this is the first and only bacterially encoded actin-binding protein that has been shown to influence actin dynamics. In addition, amino acid sequence analysis has not revealed the presence of sequences similar to known actin-binding motifs, suggesting the possibility that SipA exerts its actin-modulating function in a unique manner. We have carried out a biophysical analysis of the functional C-terminal fragment of SipA, SipA$^{446-684}$, using multiangle laser light scattering (MALLS), small angle X-ray scattering (SAXS) and circular dichroism (CD) in an effort to elucidate structural aspects of SipA$^{446-684}$ that may help the understanding of its biological activities.

2. Materials and methods

2.1. Purification of recombinant SipA protein from Escherichia coli

A fusion between glutathione-*S*-transferase (GST) and the C-terminal 226 amino acids of SipA (GST-SipA$^{446-684}$) was purified as described [7] using glutathione Sepharose 4B (Pharmacia, Piscataway,

*Corresponding author. Fax: (1)-203-737 2630.
E-mail: jorge.galan@yale.edu

[1] Present address: Department of Molecular Biophysics and Biochemistry, Yale University, 266 Whitney Ave., New Haven, CT 06520-8114, USA.

Abbreviations: MALLS, multiangle laser light scattering; SAXS, small angle X-ray scattering; CD, circular dichroism; GST, glutathione-*S*-transferase

0014-5793/00/$20.00
PII: S0014-5793(00)02040-8

NJ, USA). The SipA$^{446-684}$ fragment was released from the GST moiety by thrombin cleavage and purified away from thrombin by affinity chromatography through a benzamidine Sepharose 6B column (Pharmacia Biotech, Piscataway, NJ, USA). SipA$^{446-684}$ was further purified by size exclusion chromatography at 4°C through a Superdex 75PG column in 150 mM NaCl, 50 mM MES, pH 7.0. The purity of the resulting preparation was greater than 95% as indicated by SDS–PAGE analysis (data not shown).

2.2. Mass determination by MALLS

To determine the molecular mass of SipA$^{446-684}$, the purified protein was analyzed on an HR-10/30 Superdex-200 size exclusion column connected to ultra violet (UV), MALLS and refractive index detectors. The sample was loaded at 312 μM in 50 mM MES, 150 mM NaCl, 5 mM dithiothreitol (DTT), pH 7.0. Light scattering and differential refractometry were carried out using the Mini-Dawn and Optilab instruments of Wyatt Technology Corp. Analysis was carried out as described by Astra software [12]. Protein concentration was determined by amino acid analysis performed at the W.M. Keck Foundation Biotechnology Resource Laboratory at Yale University.

2.3. SAXS

SAXS measurements of SipA$^{446-684}$ were performed at 624 μM (15.9 mg/ml) and 312 μM (7.95 mg/ml) in 50 mM MES, 150 mM NaCl, 5 mM DTT, pH 7.0 at 25°C. The SAXS instrument and experimental methods used were as described before [13]. The X-ray beam was circularly collimated. The sample to detector distance was 2.3 m, enabling the measurement of an effective Q range of 0.015–0.30 Å. $Q = 4\pi\sin\theta/\lambda$ is the magnitude of the scattering vector, where 2θ is the scattering angle and $\lambda = 1.54$ Å is the wavelength of the X-rays. The $P(r)$ function was generated from the scattering data by the GNOM program [14]. Shape determination was performed using the program DAMMIN [15].

2.4. CD

The CD spectrum of SipA$^{446-684}$ was recorded at 25°C at a protein concentration of 7.8 μM in phosphate-buffered saline (150 mM NaCl, 16 mM Na_2HPO_4, 4 mM NaH_2PO_4). The spectrum was obtained by averaging over five scans with a step size of 1 nm and an averaging time of 4 s on an AVIV model 62DS CD spectrometer. Measurements were preformed in a Hellma quartz cuvette of path length 0.1 cm. Helix content was calculated from the molar ellipticity at 208 nm [16].

3. Results

As part of the purification process, SipA$^{446-684}$ was subjected to size exclusion chromatography, where the protein eluted at a position of higher apparent molecular mass (based on globular protein mass standards) than the mass expected from its predicted amino acid sequence (data not shown). We therefore determined the absolute molecular mass of SipA$^{446-684}$ by MALLS, a technique which does not rely on the shape of the molecule. SipA$^{446-684}$ eluted as a monomeric species of molecular mass 24 kDa (Fig. 1) which is in good agreement with the molecular mass determined by mass spectrometry (25.6 kDa, data not shown). To reconcile the size exclusion chromatography results with the MALLS results, we performed SAXS measurements on SipA$^{446-684}$. SAXS measures molecular weight, size and shape of a molecule, and gives information about the global conformation of a protein in solution. Two protein concentrations were used: 15.9 mg/ml and 7.95 mg/ml. The average radius of gyration, R_g, obtained from both the Guinier approximation (Fig. 2A) and the length distribution function $P(r)$ (Fig. 2B) was 27 Å from measurements at both concentrations (Fig. 2 shows the results for [SipA$^{446-684}$] = 15.9 mg/ml). The skewed shape of the $P(r)$ function for SipA$^{446-684}$ suggests an elongated shape, which is corroborated by the maximum diameter (D_{max}) of

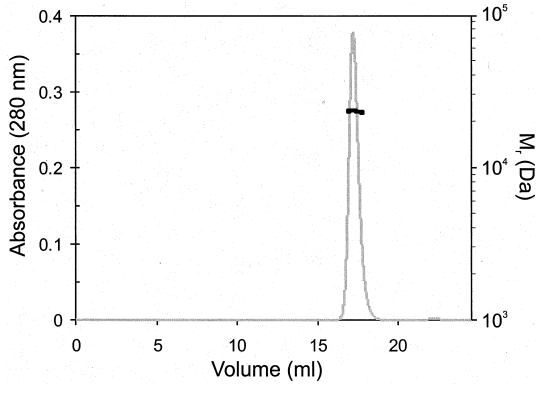

Fig. 1. Molecular mass determination by MALLS. In gray (left axis) is shown the UV absorption profile at 280 nm and in black (right axis) the molecular mass as determined by MALLS using the protein concentration calculated by the refractive index.

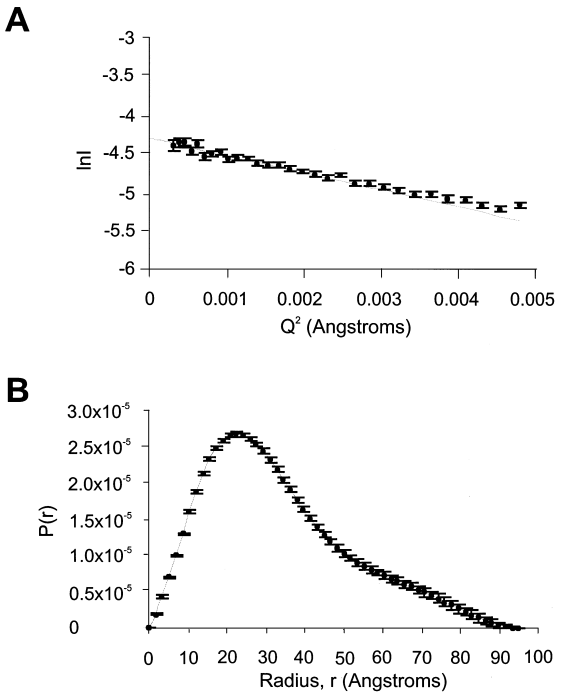

Fig. 2. Shape determination of SipA$^{446-684}$ by SAXS. Data are shown for a SipA$^{446-684}$ concentration of 624 μM (15.9 mg/ml). (A) Guinier plot of SipA$^{446-684}$. (B) Length distribution function, $P(r)$, of SipA$^{446-684}$.

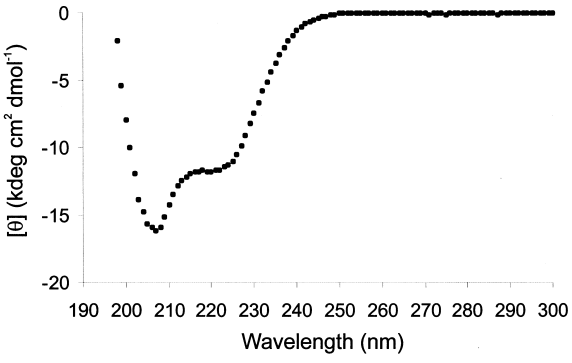

Fig. 3. CD spectrum of SipA$^{446-684}$.

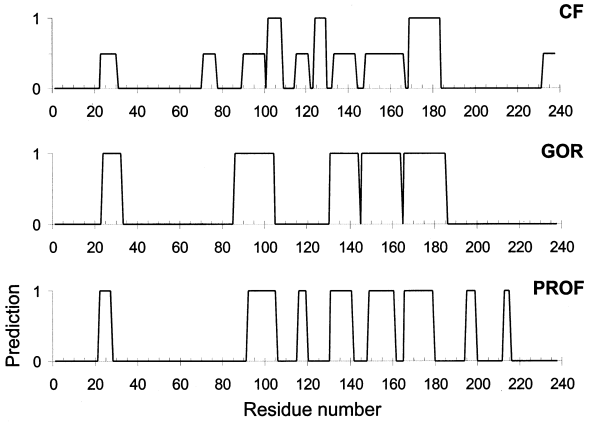

Fig. 4. Secondary structure prediction of SipA$^{446-684}$. The top two panels show the probability of occurrence of α-helical secondary structure as predicted by the Chou and Fasman method (CF, top panel) and Garnier–Osguthorpe–Robson method (GOR, middle panel) of the Wisconsin Package Version 10.0, Genetics Computer Group (GCG) [19]. In the top panel, weaker probabilities have a prediction value of 0.5 and strong probabilities a value of 1. The last panel (PROF) shows the probability of helical secondary structure according to the Prof method developed by Ouali, M. and King, R.D [20].

95 Å. As a reference, the theoretical R_g of a monomeric globular protein of molecular mass 25.6 kDa is 12.4 Å with a maximum diameter of 39.2 Å. The R_g of a long uniform rod of length 95 Å is 27 Å. The scattering data for SipA$^{446-684}$ were also run through a shape determination program (DAMMIN [15]), which yielded an elongated, roughly cylindrically shaped molecule with end-to-end lengths ranging between 85 and 95 Å and diameters ranging between 15 and 25 Å.

A good candidate for a stable protein with an elongated shape is one with a coiled-coil domain composed of two or more helices. To test this idea, we determined the CD spectrum of SipA$^{446-684}$ (Fig. 3), which shows significant α-helical content, indicated by the characteristic double minimum at 208 and 222 nm. SipA$^{446-684}$ is about 54% helical, which corresponds to 127 residues. The protein sequence was run through secondary structure prediction programs, which predicted a predominantly helical conformation for residues 93–216, a span of 123 residues, and residues 25–30. To be 95 Å in length, a standard α-helix must contain 63 amino acids. The biophysical and secondary structure prediction data for SipA$^{446-684}$ (Fig. 4) support the existence of a coiled-coil domain composed of two antiparallel helices, each consisting of about 60 residues, which span a length of 95 Å.

4. Discussion

F-actin can be viewed either as a left-handed single helix with a rise per monomer of 27.5 Å and 13 subunits that repeat after six turns or as a right-handed double helix with a rise per monomer on each helix strand of 55 Å and a repeat every 72 nm [17]. The maximum diameter of the filament varies between 90 and 95 Å. Given the highly elongated nature of SipA$^{446-684}$, it is possible that the protein spans two neighboring actin monomers in a filament. Any potential modelling of this interaction should take into account the previous finding that binding to F-actin occurs in a 1:1 molar ratio of SipA$^{446-684}$ to actin monomer and the observation that

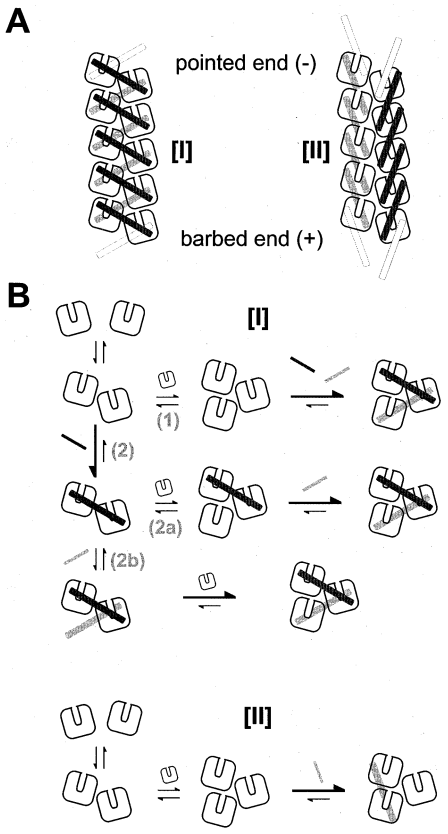

Fig. 5. Possible models of SipA$^{446-684}$ action on F-actin. (A) Shown is an unwound portion of F-actin, where actin monomers are drawn as rounded squares with a groove indicating the nucleotide-binding site. The rigid domain of SipA$^{446-684}$, which contains a coiled-coil domain of length 95 Å consisting of two antiparallel helices, is shown as an elongated rod. In model [I], SipA$^{446-684}$ spans two adjacent actin monomers across the double-stranded helix both in the front (dark gray) and in the back (light gray). Model [II] shows SipA$^{446-684}$ spanning two consecutive actin monomers in the same strand. SipA$^{446-684}$ molecules might bind to the pointed and/or barbed end in either model (dashed, unfilled rods). (B) SipA$^{446-684}$ may decrease the actin critical concentration necessary for filament formation by shifting the equilibrium towards the trimeric actin nucleus. This could occur by multiple pathways for model [I], depending on whether SipA$^{446-684}$ binds the dimeric actin, and also on the sequence of SipA$^{446-684}$ and actin monomer binding to the actin dimer. For model [II] one SipA$^{446-684}$ molecule is shown binding to the trimer after it has formed.

SipA$^{446-684}$ is monomeric and thus does not bind to itself. Two models of how SipA$^{446-684}$ might interact with F-actin are depicted in Fig. 5A. In model [I], SipA$^{446-684}$ binds adjacent actin monomers across the double-stranded right-handed helix on both faces and predicts a SipA$^{446-684}$ to actin monomer ratio of $n-1:n$, which for long filaments is essentially 1:1. If SipA$^{446-684}$ molecules also bind with one end to the last actin monomer at the pointed and/or barbed end, the predicted molar ratio changes to $n:n$ or $n+1:n$. A rigid coiled-coil domain spanning actin monomers across the double-stranded filament helix would ensure rigidity and stabilization of the filament. This is in accordance with the straightening out phenomenon observed for F-actin filaments in the presence of SipA$^{446-684}$ and the inhibition of F-actin depolymerization at low ionic strength. In model [II], SipA$^{446-684}$ is shown binding to two consecutive actin monomers in the

same strand of the double-stranded filament helix, giving a predicted SipA$^{446-684}$ to actin molar ratio of $n-2:n$. If upto four additional SipA$^{446-684}$ molecules bind to the barbed and pointed ends, the binding ratio could vary from $n-1:n$ to $n+2:n$. In this model, stabilization of the filament by SipA$^{446-684}$ could occur by inducing conformational changes in the actin, such that interactions across the two strands of the double helix are strengthened, consequently stabilizing the filament overall. It should be noted that both models imply the presence of more than one actin-binding site on SipA$^{446-684}$ and consequently two or more SipA$^{446-684}$ binding sites on each actin monomer. Fig. 5B attempts to account for the decrease in actin critical concentration by SipA$^{446-684}$, which could be a consequence of stabilization of the trimeric actin nucleus [18]. This would shift the equilibrium from monomer to oligomer, thereby lowering the critical concentration. For model [I] several pathways of stabilization of the nucleus are conceivable. It has been observed that SipA$^{446-684}$ does not bind to monomeric actin [7], suggesting that either SipA$^{446-684}$ binds to and stabilizes an actin dimer (2) and subsequently the trimeric actin nucleus or that SipA$^{446-684}$ directly stabilizes the trimeric actin nucleus (1) without binding an actin dimer. Pathway (2) has two possible branches depending on the order of SipA$^{446-684}$ and actin monomer binding to the stabilized dimer. In (2a) actin binds first and the trimer is further stabilized by binding a SipA$^{446-684}$ molecule, whereas in (2b) another SipA$^{446-684}$ molecule binds to the stabilized dimer to which an actin monomer subsequently binds. For model [II] only one SipA$^{446-684}$ stabilizes the trimeric actin nucleus, after it has formed. We have synthesized the biophysical data describing structural characteristics of SipA$^{446-684}$ into two possible models, which are consistent with the biochemical effects of SipA$^{446-684}$ on actin. Although both models are consistent with the biophysical data described here, model [I] might explain better and more simply how SipA$^{446-684}$ lends stability to F-actin than does model [II]. Future mutagenesis mapping to determine binding sites, detailed analysis of the stoichiometry of SipA$^{446-684}$ binding to filaments of different lengths, in depth study of the binding of SipA$^{446-684}$ to actin nuclei and structural studies will be needed to corroborate either of the models presented here.

Acknowledgements: We thank the Natural Science and Engineering Research Council of Canada for providing K.M. with a PGS fellowship. This work was carried out in the laboratories of D.M. Engelman and T.A. Steitz in the Department of Molecular Biophysics and Biochemistry at Yale University and funded in part by Public Health Service Grant GM22778 and GM52543 from the National Institutes of Health.

References

[1] Galán, J.E. and Bliska, J.B. (1996) Ann. Rev. Cell Dev. Biol. 12, 219–253.
[2] Galán, J.E. (1999) Curr. Opin. Microbiol. 2, 46–50.
[3] Galán, J.E. and Collmer, A. (1999) Science 284, 322–328.
[4] Hardt, W.-D., Chen, L.-M., Schuebel, K.E., Bustelo, X.R. and Galán, J.E. (1998) Cell 93, 815–826.
[5] Fu, Y. and Galan, J.E. (1999) Nature 401, 293–297.
[6] Norris, F.A., Wilson, M.P., Wallis, T.S., Galyov, E.E. and Majerus, P.W. (1998) Proc. Natl. Acad. Sci. USA 95, 14057–14059.
[7] Zhou, D., Mooseker, M. and Galán, J.E. (1999) Science 283, 2092–2095.
[8] Chen, L.M., Hobbie, S. and Galán, J.E. (1996) Science 274, 2115–2118.
[9] Chen, L.M., Bagrodia, S., Cerione, R.A. and Galán, J.E. (1999) J. Exp. Med. 189, 1479–1488.
[10] Zhou, D., Chen, L.-M., Shears, S. and Galán, J.E. (2000) (submitted).
[11] Zhou, D., Mooseker, M.S. and Galán, J.E. (1999) Proc. Natl. Acad. Sci. USA 96, 10176–10181.
[12] Wyatt, P. (1993) Anal. Chim. Acta 272, 1–40.
[13] Bu, Z. (1998) J. Appl. Cryst. 31, 533–543.
[14] Semenyuk, A.V. and Svergun, D.I. (1991) J. Appl. Cryst. 24, 537–540.
[15] Svergun, D. (1999) Biophys. J. 76, 2879–2886.
[16] Greenfield, N. and Fasman, G.D. (1969) Biochemistry 8, 4108–4116.
[17] Holmes, K.C., Popp, D., Gebhard, W. and Kabsch, W. (1990) Nature 347, 44–49.
[18] Wegner, A. (1976) J. Mol. Biol. 108, 139–150.
[19] Jameson, B.A. and Wolf, H. (1988) Comput. Appl. Biosci. 4, 181–186.
[20] Ouali, M. and King, R.D. (2000) (in press).